PHYSICAL REVIEW A **76**, 051803(R) (2007)

Sub- and superdiffractive resonators with intracavity photonic crystals

K. Staliunas,[1] M. Peckus,[2] and V. Sirutkaitis[2]
[1]*Institució Catalana de Recerca i Estudis Avançats (ICREA), Departament de Física i Enginyeria Nuclear, Universitat Politècnica de Catalunya, Colom 11, 08222 Terrassa, Spain*
[2]*Laser Research Center, Vilnius University, Sauletekio al 10, LT-10222 Vilnius, Lithuania*
(Received 17 August 2007; published 26 November 2007)

We investigate experimentally and theoretically plane-mirror Fabry-Perot resonators filled by photonic crystals, i.e., with periodic intracavity refraction index modulation. We show that the diffraction properties of such resonators can be manipulated, resulting in sub- and superdiffractive dynamics of light in the resonator, and in hyperbolic angular transmission profiles.

DOI: 10.1103/PhysRevA.76.051803 PACS number(s): 42.55.Tv, 42.25.Fx, 42.79.−e

Photonic crystals (PCs), the materials with periodic in space refraction index, is an object of intensive study since their proposal in 1987 [1–3]. The studies were focused initially on the *temporal* dispersion characteristics of the PCs. The dispersion curves were found to modify substantially due to the periodic modulation of the index, and to display a band structure—a most celebrated feature of the PCs. More recently it was found that the *spatial* dispersion (diffraction) characteristics also modify substantially in periodic materials: the diffraction can become negative [4,5], or can vanish to zero [6–10], resulting in the so-called self-collimation effect in the latter case.

Diffraction manipulation affects primarily the linear propagation of light beams in bulk PCs [4–10]. However, diffraction manipulation can also create phenomena in more complicated systems based on PCs. In particular, the periodic index modulation in Kerr-nonlinear materials leads to the nonlinear formations of light, such as band gap solitons [11], subdiffractive solitons [12], and others. Periodic index modulation in quadratic nonlinear materials leads to modification of the spatial phase matching profile [13]. The present work is based on the idea that the periodic modulation of the index can also substantially alter the properties of the *resonator* filled by such material. As the transverse and longitudinal mode structure, and also the angular transmission profile of the resonator is dependent on its diffraction, then these characteristics can alter substantially due to the manipulation of diffraction.

Figure 1 illustrates the basic idea. The mode structure of the resonator follows from the resonance condition for the longitudinal component of the wave vector, $k_{\parallel,m}=2\pi m/(2l)$ (m is the longitudinal mode number and l is the linear cavity length). The transverse wave numbers in resonance in the plane mirror (Fabry-Perot) resonator are $k_\perp=\sqrt{|\mathbf{k}|^2-k_{\parallel,m}^2}$, as illustrated in Fig. 1(a), resulting in a system of concentric Fresnel rings in the resonator angular transmission profile. As the diffraction in PCs is modified, then the angular transmission profile changes too [see Fig. 1(b)]. It can be expected, in particular, that the central part of the transmission profile could be relatively homogeneous in the case shown in Fig. 1(b).

The aim of this paper is to explore the mode structure and the angular transmission profile of the plane-mirror resonator filled by two-dimensional (2D) PCs. We concentrate on the parameters corresponding to the zero diffraction point, where the spatial dispersion curves develop flat segments [10]. We investigate two parameter regions. (1) When the flat segment is relatively broad, this results in a relatively broad angular spectrum supported by the resonator, corresponding to relatively fine near-field spatial structures. We call this region subdiffractive. (2) When the flat segment is relatively narrow, this results in a relatively narrow angular spectrum, corresponding to relatively clean near-field spatial structures. We call this region superdiffractive. The limit between these two regions is specified below.

For experiments the resonator was fabricated considering that the nondiffractive propagation in the first propagation band occurs along the diagonal direction of the square—or the rhombic lattice of the PC [4–10]. The resonator used in experiments is shown schematically in Fig. 2(a). In order to achieve the effect of 2D intracavity index modulation the surfaces of the mirrors were first covered with a thin film of Shipley photoresist (of $\propto 0.4$ μm thickness, of $n=1.58$ index of refraction) using spin coating technique. Next, using photolithography technology, the 1D periodic structure was

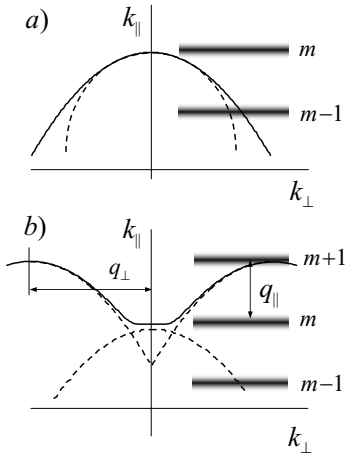

FIG. 1. Longitudinal and transverse mode structure of homogeneous resonators (a), and of the resonators with manipulated (eliminated) diffraction (b). The case (b) is calculated from Eq. (4) with $L=9.5$, $f=0.07$. The dashed line [half circle in (a)] indicates the spatial dispersion curve without paraxial approximation. The dashed lines in (b) indicate the dispersion curves in the limit of vanishing index modulation ($f\to 0$).

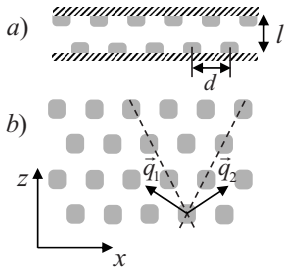

FIG. 2. The scheme of the resonator used in experiments (a), and the corresponding unfolded PC structure (b). The dashed lines indicate crystallographic axes of the unfolded PC structure, and the arrows represent the vectors of the reciprocal lattice.

etched on the layers of the film of photoresist with the period $d=15$ μm (the width of the etched groves was approximately half of their period $\propto d/2$), so the coatings on the mirror act as the phase grating. The distance between the mirrors (the linear length of the resonator) was varied in the range of $l=0.2-1.0$ mm. The mirrors were shifted one with respect to another by the half of the grating period in order to mimic the 2D photonic crystal with the optical axis directed along the diagonals of rhombs [see Fig. 2(b) for the unfolded structure of the resonator]. In this way the radiation in a round trip along the resonator "sees" exactly one longitudinal period of the unfolded PC. The resonator was illuminated by the cw laser beam (wavelength 532 nm, beam width 2.5 mm, power 15 mW). A diffuser was placed at a distance of 40 mm in front of the front mirror of the resonator in order to generate a broad spatial spectrum of the illuminating radiation. A lens of 58 mm focal distance was used to collect the transmitted radiation into charge-coupled device (CCD) camera for the far field recording.

Theoretical analysis of the resonator is based on the unfolded structure of the modulated resonator [Fig. 2(b)], with the refraction index periodic in the x (transversal) and z (longitudinal) directions with the corresponding periods d and $2l$. We use a paraxial model of the PC,

$$\partial_Z A(\mathbf{r}) = i[\nabla_\perp^2 + V(\mathbf{r})]A(\mathbf{r}), \tag{1}$$

where $\nabla_\perp^2 = \partial^2/\partial X^2 + \partial^2/\partial Y^2$ is the Laplace operator in the transverse plane. The transverse coordinates X, Y are normalized to $x_0 = d/2\pi$ in order to make the normalized transverse wave number of the index grating equal to unity $q_\perp = 1$. The longitudinal coordinate is normalized to $z_0 = 2|\mathbf{k}|x_0^2$ in order to make the coefficient of diffraction equal to one. The longitudinal period of the index grating in the normalized coordinates Z is then $L = l(2\pi)^2/(|\mathbf{k}|d^2)$ and the corresponding modulation wave numbers is $q_\parallel = 2\pi/L = d^2/(\lambda l)$. $V(\mathbf{r}) = 2x_0^2 n(\mathbf{r})$.

We expand the intracavity field into a set of plane waves,

$$A(\mathbf{r}) = e^{i(k_x X + k_y Y)} \sum_{m,n} a_{m,n}(Z) e^{i(mX - nq_\parallel Z)}. \tag{2}$$

Substitution of Eq. (2) into Eq. (1) yields the equation system

$$\partial_z a_{m,n} = -i[(m+k_x)^2 + k_y^2 - nq_\parallel]a_{m,n} + if_{m,n} \sum_{p\neq m, q\neq n} a_{p,q} \tag{3}$$

for the amplitudes of the plane waves $a_{m,n}$. Here $f_{m,n}$ is the matrix of the coupling coefficients depending on the character of the modulation of the index: $f_{m,n} = c^{-1} \int V(\mathbf{r}) e^{-i(mX - nq_\parallel Z)} d\mathbf{r}$, as integrated over the unitary cell of the PC, c being the area of the cell.

Only three central harmonics in the expansion (2) are relevant for the sub- and superdiffractive propagation in the PC (see, e.g., [10,12]), and consequently for the sub- and superdiffractive dynamics of the resonator. We therefore rewrite Eq. (3) in terms of the vector of the amplitudes of plane waves, $\mathbf{A} = \{a_{-1,1}, a_0, a_{11}\}$. In the limit of zero coupling (zero index modulation) these are the waves propagating with the wave vectors $(k_\perp - 1, k_\parallel + q_\parallel)$, $(k_\perp, k_\parallel)$, and $(k_\perp + 1, k_\parallel + q_\parallel)$, as shown by the dashed lines in Fig. 1(b). The integration of Eq. (3) over one longitudinal period of the PC (equivalently over one resonator round trip) leads to the mapping

$$\mathbf{A}(Z+L) = e^{(\mathbf{P}+\mathbf{F})L}\mathbf{A}(Z), \tag{4}$$

where $\mathbf{P}$ is a diagonal propagation matrix with the elements $[-i(k_\perp - 1)^2 + iq_\parallel, -ik_\perp^2, -i(k_\perp + 1)^2 + iq_\parallel]$, and $\mathbf{F}$ is the off-diagonal scattering matrix. We consider that only the next-to-diagonal elements of $\mathbf{F}$ are nonzero ($f_{m,n} = f$ for $|m-n| = 1$, otherwise $f_{m,n} = 0$), as obtained by calculating the above integral, as well as guided by the experimental measurements of the scattering from one modulated mirror. The results, however, are qualitatively weakly dependent from the exact form of the matrix $\mathbf{F}$.

We calculate the diffractive propagation through the unfolded PC by diagonalizing the propagation and the scattering matrix $\mathbf{P}+\mathbf{F}$. The imaginary part of the eigenvalues yields the spatial dispersion relation $k_\parallel(k_X, k_Y)$, which allows us to calculate the angle-dependent phase shift of the Bloch modes over the longitudinal PC period $\Delta\varphi(k_X, k_Y) = Lk_\parallel(k_X, k_Y)$. Figure 1(b) shows the spatial dispersion relation on cross section $k_y = 0$ calculated at a zero diffraction point. The initially parabolic segments of the individual dispersion curves (for each of the harmonics) interact due to the modulation (coupling) and repel one another at their crossing point. The dispersion curve disshapes, and at the zero diffraction point attains a flat segment. It is evident from Fig. 1 that the zero diffraction occurs close to (but not exactly at) the point of the triple intersection of the spatial dispersion curves [parabolas in Fig. 1(b)] at $L = 2\pi$ $(q_\parallel \to 1)$. The parabolas must be slightly separated from the triple intersection point to form the flat segments, with the separation distance depending on the scattering strength f.

Asymptotic analysis allows the estimation of the localization of the zero diffraction point. In the limit of weak scattering $f \ll 1$, also near to the triple intersection point, the spatial dispersion curve [the imaginary part of the eigenvalue of Eq. (4)] can be obtained as the series expansion at the point $k_x = k_y = 0$,

$$k_{\parallel}(k_X,k_Y) = D_0 - D_2k_X^2 - k_Y^2 - D_4k_X^4 + O(k_X^6) \quad (5)$$

(see, e.g., [10,12] for scalings). Here $D_0=2f^2/(1-q_{\parallel})$ is the uniform shift of the wave number due to the modulation of refractive index; $D_2=1-8f^2/(1-q_{\parallel})^3$ is the first (leading) order diffraction coefficient, which is tuned to zero at $8f^2=(1-q_{\parallel})^3$; $D_4=32f^2/(1-q_{\parallel})^5$ describes the second-order diffraction, which becomes dominant at—or close to—the zero diffraction point. The spatial dispersion surface (5) has a single maximum in the normal diffraction regime $[8f^2<(1-q_{\parallel})^3]$; however, it is of saddle shape in the case of negative or zero diffraction.

Next, in order to consider the resonator effects, the mapping (4) is modified. The partial transmission of the mirrors is accounted for by the diagonal matrix with the elements $t^2:t^2\mathbf{1}$, where $\mathbf{1}$ is the unit matrix, and t denotes the transmission of a mirror (the resonator consisting of two identical mirrors was considered). The resonator phase shift is accounted for by the term $e^{i\varphi\mathbf{1}}$. The incident light is accounted for by adding the vector $\mathbf{A}_0=(0,t,0)$ at every resonator round trip. We consider for simplicity the near-to-resonance limit, also a good finesse cavity limit, implying a weak scattering in the PC structure, and highly reflecting mirrors of the resonator. This allows us to simplify the propagation operator in Eq. (4) by expanding it in series $e^{(\mathbf{P}+\mathbf{F})L+i\varphi\mathbf{1}}\approx\mathbf{1}+(\mathbf{P}+\mathbf{F})L+i\varphi\mathbf{1}+\ldots$. We calculate the resonator transmission in an analogous way as the transmission of the homogeneously filled plane-mirror Fabry-Perot resonator; however, we manipulate with the vector $\mathbf{A}$ of the plane wave components. We required that the radiation does not alter in a one resonator round trip,

$$\mathbf{A}(0) = \mathbf{A}(L) = [\mathbf{1}(1-t^2+i\varphi) + (\mathbf{P}+\mathbf{F})L]\mathbf{A}(0) + \mathbf{A}_0. \quad (6)$$

Then the resonator transmission is given by

$$\mathbf{R} = [\mathbf{1}(t^2 - i\varphi) - (\mathbf{P}+\mathbf{F})L]^{-1}\mathbf{T}. \quad (7)$$

The element R_{22} of the resonator transmission matrix (7) yields the transmission of the central component of the resonator. We calculate the transmission of the resonator at the zero diffraction point numerically, using Eq. (7), both in the sub- and superdiffraction regimes (see Fig. 3). Figures 3(a) and 3(b) represent the subdiffraction limit, where the angular transmission function is broadened in the direction of index modulation (X direction), as compared to transmission in the homogeneous (Y) direction. This case corresponds to the relatively broad plateau of the manipulated spatial dispersion. Figures 3(c)–3(e) represent the opposite limit, when the dispersion curve develop relatively narrow plateau, resulting in superdiffraction or, equivalently, the resonator shows the filtering function. In both cases the formation of strongly anisotropic (of hyperbolic form) angular transmission distributions is obtained. The parameters used for Figs. 3(c)–3(e) were chosen to correspond to our experiment reported below.

We evaluate the boundary between the sub- and superdiffractive regimes of the resonator assuming that at the boundary the angular width of the resonance is equal to that of a homogeneously filled resonator. The width of the resonance at zero diffraction point is governed by second-order diffraction, and, as follows from expansion (5), is $\Delta k_{\perp}=(D_4Q)^{-1/4}$,

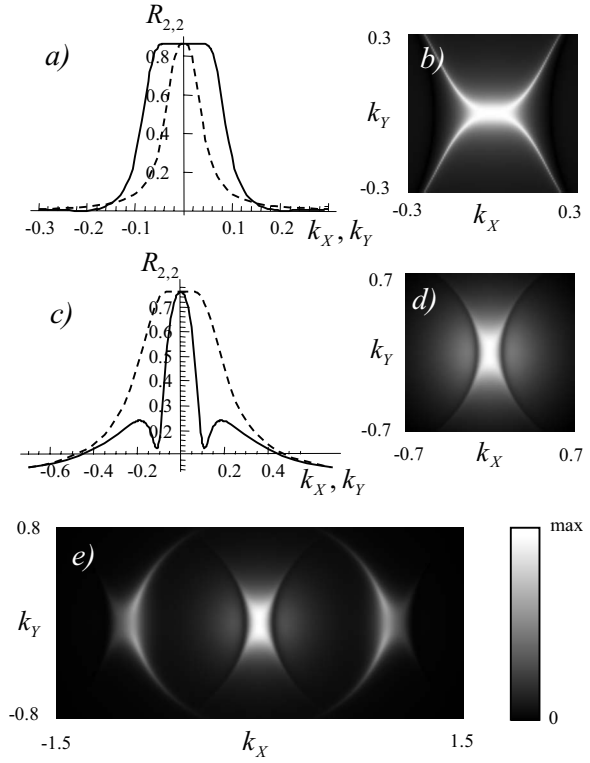

FIG. 3. The element R_{22} of the resonator transmission matrix (7): (a),(c) show transmission on the cross sections $k_Y=0$ (solid lines) and $k_Z=0$ (dashed lines). (b),(d) show 2D angular transmission profiles. (e) shows the full transmission as a sum of central transmission component R_{22} and of the first diffraction maxima R_{21} and R_{23}. Parameters for (a),(b) are $L=9.5$, $f=0.08$, $t=0.1$, $\varphi=-0.395$; for (c)–(e), $L=7.5$, $f=0.05$, $t=0.44$, $\varphi=-0.35$.

where Q is the resonator finesse. The angular spectrum of the homogeneous cavity, in terms of the normalized variables, is $Q^{-1/2}$. Then the boundary between the sub- and superdiffraction regimes is given by $D_4=Q$, or, equivalently, by $fQ^{3/4}=1$. A strong intracavity index modulation in high finesse resonators $(fQ^{3/4}>1)$ results in subdiffraction, whereas the opposite regime of a weak index modulation in low finesse resonators $fQ^{3/4}<1$ leads to the effect of the narrowing of the spatial spectrum, i.e., spatial filtering.

In experiments we varied the length of the resonator on a large scale in order to tune to the zero diffraction point, which, according to the theoretical calculations ($L=7.5$), was evaluated to exist at $l=0.55$ mm. (The critical point of triple interaction is at $l=d^2/\lambda=0.44$ mm.) The length of the resonator was also varied on the small (submicron) scale in order to tune the on axis radiation to the resonance. Figure 4 shows the experimentally recorded far field pattern. The central part of the experimentally obtained distribution corresponds well to the theoretically predicted hyperboliclike structure shown in Fig. 3(c). The theoretically predicted first-order diffraction maxima [Fig. 3(e)] are also observed experimentally.

Besides the theoretically predicted central transmission components, the higher order diffraction components were experimentally observed [Fig. 4(b)]. These components are beyond the scope of theoretical treatment, as related with the higher diffraction orders on the index grating. (In theoretical

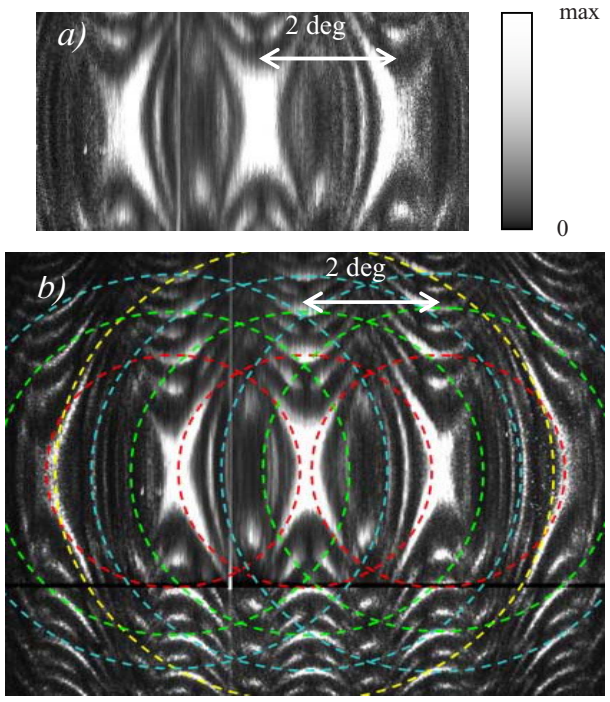

FIG. 4. (Color online) Far field of the radiation transmitted through the resonator recorded experimentally: (a) The central part of the transmitted distribution (corresponding to calculated distribution). (b) Full spatial spectrum, containing higher harmonics and different longitudinal modes. The dashed circles indicate the resonator resonance rings, and the shifted (due to the lateral index modulation) resonance rings.

treatment based on three-mode expansion only the first diffraction orders are considered.) These components are also related with the different longitudinal modes. (In the theory the single longitudinal mode treatment is performed.) These components match with the intersections of the high-order diffraction rings of the resonator, as indicated by the dashed circles in Fig. 4(b).

Concluding, we built the resonator with the intracavity modulation of refraction index, i.e., the resonator containing one longitudinal period of the PC. We developed the theory of such a resonator, predicting the sub- and superdiffractive regimes. We demonstrated experimentally the basic properties expected, i.e., the superdiffraction in the transverse direction of index modulation, as well as 2D hyperboliclike transmission patterns. The available sample with relatively low index modulation ($f \approx 0.05$) and relatively low finesse ($Q \approx 10$) allowed to realize experimentally the superdiffractive regimes only.

The resonators investigated here can be utilized to observe also the nonlinear effects. The studies of nonlinear effects in diffraction manipulated systems have been initiated (hyperbolic patterns in optical systems [14], and in Bose-Einstein condensates [15]). Also the nonlinear effects in resonators with the index modulated in transverse direction only were investigated (in 1D PCs in resonators with $\chi^{(2)}$ [16] and $\chi^{(3)}$ [17,18] nonlinearities) predicting the modification of instabilities. The nonlinear resonators with 2D photonic crystals, however, have never been investigated up to now. In particular the significant narrowing of the nonlinear structures (e.g., spatial solitons) in subdiffractive regimes, and a significant enhancement of spatial stability of these structures in superdiffractive (filtering) regimes, can be anticipated.

The work was financially supported by the Ministerio de Educación y Ciencia (Spain) through Project No. FIS2005-07931-C03-03, and the Lithuanian Ministry of Sciences through Project No. BPD2004-ESF-2.5.0-03-05/0055. We acknowledge the Institute of Physical Electronics of Kaunas Technology University and also Altechna Ltd for fabrication of the mirrors.

[1] E. Yablonovitch, Phys. Rev. Lett. **58**, 2059 (1987).
[2] S. John, Phys. Rev. Lett. **58**, 2486 (1987).
[3] R. Zengerle, J. Mod. Opt. **34**, 1589 (1987).
[4] H. S. Eisenberg, Y. Silberberg, R. Morandotti, and J. S. Aitchison, Phys. Rev. Lett. **85**, 1863 (2000).
[5] R. Morandotti, H. S. Eisenberg, Y. Silberberg, M. Sorel, and J. S. Aitchison, Phys. Rev. Lett. **86**, 3296 (2001).
[6] H. Kosaka *et al.*, Appl. Phys. Lett. **74**, 1212 (1999).
[7] T. Pertsch, T. Zentgraf, U. Peschel, A. Brauer, and F. Lederer, Phys. Rev. Lett. **88**, 093901 (2002).
[8] D. N. Chigrin *et al.*, Opt. Express **11**, 1203 (2003).
[9] R. Illiew *et al.*, Appl. Phys. Lett. **85**, 5854 (2004).
[10] K. Staliunas and R. Herrero, Phys. Rev. E **73**, 016601 (2006).
[11] M. J. Ablowitz and Z. H. Musslimani, Phys. Rev. Lett. **87**, 254102 (2001).
[12] K. Staliunas, R. Herrero, and G. J. de Valcarcel, Phys. Rev. E **73**, 065603(R) (2006).
[13] K. Staliunas *et al.*, Opt. Lett. **32**, 1992 (2007).
[14] K. Staliunas and M. Tlidi, Phys. Rev. Lett. **94**, 133902 (2005).
[15] C. Conti and S. Trillo, Phys. Rev. Lett. **92**, 120404 (2004).
[16] D. Gomila, R. Zambrini, and G. L. Oppo, Phys. Rev. Lett. **92**, 253904 (2004).
[17] D. Gomila and G. L. Oppo, Phys. Rev. E **72**, 016614 (2005).
[18] A. G. Vladimirov *et al.*, Opt. Express **14**, 1 (2006).